Available online at www.sciencedirect.com

ScienceDirect

Solar Energy 125 (2016) 207–218

SOLAR ENERGY

www.elsevier.com/locate/solener

New theoretical modelling of heat transfer in solar ponds

Assad H. Sayer [a,b,*], Hazim Al-Hussaini [a], Alasdair N. Campbell [a]

[a] Department of Chemical and Process Engineering, Faculty of Engineering and Physical Sciences, University of Surrey, GU2 7XH, UK
[b] University of Thi-Qar, College of Science, Chemistry Department, Thi-Qar, Iraq

Received 11 July 2015; received in revised form 4 October 2015; accepted 3 December 2015

Communicated by: Associate Editor Aliakbar Akbarzadeh

Abstract

Solar energy has a promising future as one of the most important types of renewable energy. Solar ponds can be an effective way of capturing and storing this energy. A new theoretical model for a heat transfer in a salinity gradient solar pond has been developed. The model is based on the energy balance for each zone of the pond; three separate zones have been considered, namely the upper convective zone, the lower convective zones, as well as the non-convective zone. The upper and lower zones are considered to be well mixed, which means the temperatures in these zones are uniform. The model shows that the temperature in the storage zone can reach more than 90 °C during the summer season whereas it can be more than 50 °C in winter if the pond is located in the Middle East. In addition, the time dependent temperature for the three layers has been found. Furthermore, it is concluded that heat loss from the pond's surface occurs mainly by evaporation, in comparison to convection and radiation. Heat loss to the ground has been calculated by using three different equations. It was found that the perimeter of the pond has a significant effect on heat loss to the ground from a small pond, while its effect is small in the case of large pond. The validity of the model is tested against experimental data for several established ponds; good agreement is observed.

Keywords: Solar pond; Solar energy; Solar storage

1. Introduction

Scientists are worried about the high levels of pollutants and they are seeking alternative sources of energy. The best alternatives to the traditional sources of energy are renewable energies; they are clean and have sustainable resources. Many different types of these energies have been used, such as wind energy, bio-energy and solar energy. Solar ponds were discovered as a natural phenomenon in Transylvania by Kalecsinsky when he presented measurements on Lake Medve. The temperature in summer was around 60 °C at a depth of 1.3 m; the sodium chloride concentration at the bottom was found to be near saturation. Interestingly, there was fresh water in the surface layer. Kalecsinsky concluded that artificial solar ponds might be useful for heat collection and storage. Significant research effort began in the 1960s, mostly concerned with generating electricity using the heat from the ponds (Nielsen, 1975). In 1977, a 1500 m^2 pond was constructed to generate 6 kW of electricity by a turbine operating a Rankine cycle. A pond of area 6250 m^2 in Ein Boqeq was built in the same year to generate 150 kW of electricity (Weinberg and Doron, 2010). In 1983, the El Paso solar pond was established and it has been in operation since

* Corresponding author at: Department of Chemical and Process Engineering, Faculty of Engineering and Physical Sciences, University of Surrey, GU2 7XH, UK. Tel.: +44 1483686562.
E-mail addresses: a.h.sayer@surrey.ac.uk (A.H. Sayer), h.al-hussaini@surrey.ac.uk (H. Al-Hussaini), a.n.campbell@surrey.ac.uk (A.N. Campbell).

http://dx.doi.org/10.1016/j.solener.2015.12.015
0038-092X/

Nomenclature

A_b	area of the bottom surface of the pond (m^2)
A_l	surface area of the LCZ (m^2)
A_u	surface area of the UCZ (m^2)
a	constant (0.36), Eq. (4)
b	constant (0.08), Eq. (4)
CCSGSP	closed cycle salt gradient solar pond
C_s	humid heat capacity of (kJ/kg K)
c_{pl}	heat capacity of water in the LCZ (J/kg K)
c_{pu}	heat capacity of water in the UCZ (J/kg K)
D_g	distance between the bottom insulation and the water table (m)
D_i	thickness of the bottom insulation (m)
E	pond's efficiency
EP	evaporation pond
F_r	refraction parameter
H	solar radiation (W/m^2)
h_c	convective heat transfer coefficient to the air (W/m^2 K)
h_x	fraction of solar radiation that reaches a depth x (W/m^2)
h_o	heat transfer coefficient from outside wall surface to the atmosphere (W/m^2 K)
h_1	heat transfer coefficient between the NCZ and the UCZ (W/m^2 K)
h_2	heat transfer coefficient between the LCZ and the NCZ (W/m^2 K)
h_3	heat transfer coefficient between the LCZ with surface at the bottom of the pond (W/m^2 K)
h_4	heat transfer coefficient at the surface of the ground water sink (W/m^2 K)
k_g	thermal conductivity of the soil under the pond (W/m K)
k_w	thermal conductivity of water (W/m K)
k_1	thermal conductivity of the first layer of insulation (W/m K)
k_2	thermal conductivity of polystyrene (W/m K)
k_3	thermal conductivity of wood (W/m K)
LCZ	lower convective zone
l_1	thickness of the first layer of insulation (m)
l_2	thickness of polystyrene layer (m)
l_3	thickness of third layer of insulation (m)
m	empirical parameter, Eq. (26)
NCZ	non-convective zone
p	pond perimeter (m)
p_a	the partial pressure of water vapour in the ambient temperature (mmHg)
p_{atm}	atmospheric pressure (mmHg)
p_u	water vapour pressure at the upper layer temperature (mmHg)
Q_{ground}	heat loss to the ground (W/m^2)
Q_{load}	heat extracted from the LCZ (W/m^2)
Q_{loses}	overall heat loss from the surface of the pond (W/m^2)
Q_R	heat absorbed in any layer of the NCZ from solar radiation (W/m^2)
Q_{rin}	solar radiation entering the UCZ (W/m^2)
Q_{rout}	solar radiation exiting the UCZ (W/m^2)
Q_{rs}	the solar radiation which enters and is stored in the LCZ (W/m^2)
Q_{ru}	solar radiation that is absorbed in the NCZ (W/m^2)
Q_{ub}	heat transfer by conduction to the UCZ (W/m^2)
Q_{uc}	convective heat loss from the surface (W/m^2)
Q_{ue}	evaporative heat loss from the surface (W/m^2)
Q_{ur}	radiation heat loss from the surface (W/m^2)
Q_w	heat loss through walls of the pond (W/m^2)
T_a	average of the ambient temperature (°C)
T_g	temperature of water table under the pond (°C)
T_k	sky temperature
T_s	temperature of the LCZ (°C)
T_u	temperature of the UCZ (°C)
t	time (s)
UCZ	upper convective zone
U_{ground}	over all heat transfer coefficient to the ground (W/m^2 K)
U_t	overall heat transfer coefficient (W/m^2 K)
X_{NCZ}	thickness of the NCZ (m)
X_l	thickness of the LCZ (m)
X_u	thickness of the UCZ (m)
x_g	distance of water table from pond's bottom (m)
x	thickness of water layer (m)

Greek letters

ϵ	emissivity of water
ρ_l	density of the LCZ
ρ_u	density of the UCZ (kg/m^3)
v	monthly average wind speed in the region of study (m/s)
λ	latent heat of vaporisation (kJ/kg)
γ_h	relative humidity
σ	Stefen–Boltzmann's constant (5.673×10^{-8} W/m^2 K^4)

1985 (Alenezi, 2012). Currently, the research on the El Paso pond is focused on coupled desalination and brine management and enhancement of the techniques of solar pond operation and maintenance (Benjamin Schober, 2010; Huanmin et al., 2004). There are two types of solar ponds, (i) convective and (ii) non-convective ponds (Alrowaished et al., 2013). A simple diagram (Fig. 1) can be drawn to demonstrate the types of solar ponds.

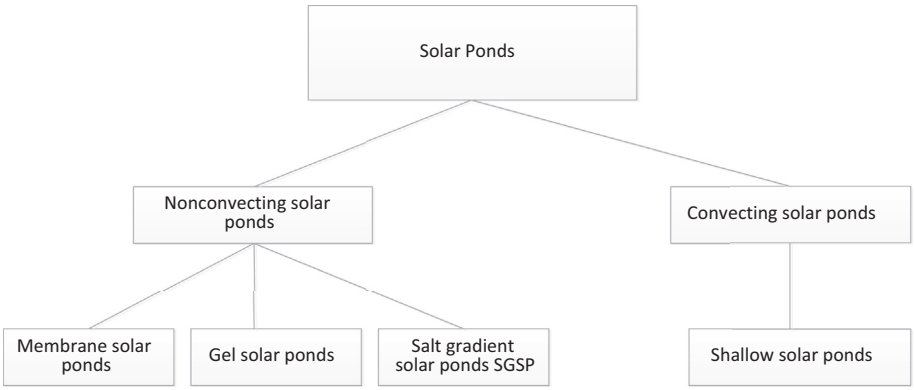

Fig. 1. Diagram showing the different classifications and types of solar ponds.

A typical convecting solar pond is the shallow solar pond. Abdelsalam (1985) described a shallow pond comprised a plastic bag made from PVC, which is clear at the top and black at the bottom to absorb radiation. A shallow solar pond has a maximum depth of 15 cm (Garg, 1987). In convective solar ponds there is no insulating zone to prevent heat losses by convection. The pond is operated under normal atmospheric conditions (Anderson, 1980).

There are several types of non-convecting solar ponds. The most important type is the salt gradient solar pond (SGSP). A salt gradient solar pond is a body of water with a depth between 2 and 5 m and a gradient of salt concentration (Leblanc et al., 2011). To prevent natural convection, salty solution is used in the SGSP. The non convecting zone (NCZ) has a salinity gradient with the salinity increasing from the top to the bottom of the layer (Velmurugan and Srithar, 2008). This will suppress, or decrease heat loss by natural convection which would be expected in fresh water. When a particular layer in the NCZ is heated, its density will decrease, but will remain higher than the layer above due to the salinity gradient. Consequently, upward movement due to buoyancy will stop, and heat can only move by conduction, from the lower layer to the top, through the NCZ (Date and Akbarzadeh, 2013). Solar ponds can take any geometrical shape. There are square, rectangular or circular cross section ponds, and the walls can also be vertical or sloping. However, a trapezoidal shape is often preferred and it is shown in Fig. 2.

Alternatives to the SGSP, which replace the insulating effect of the NCZ with either a transparent gel layer (Wilkins et al., 1982; Wilkins and Lee, 1987), or a transparent membrane (Hull, 1980) have been proposed. These alternatives have, however, received much less attention than the SGSP. In all cases, the heat from the pond can be used effectively in space heating, domestic and low temperature applications.

2. Previous theoretical models

Kooi (1979) developed a model to describe the SGSP. The steady state heat conduction equation was used to calculate the vertical temperature distribution, and an expression for the heat collected in the pond was developed. Many assumptions were adopted in the model. Firstly, it was considered that the pond's walls are vertical and well insulated. The base was also assumed to be well insulated. Secondly, the UCZ and LCZ were considered uniform with constant temperature and k_w were held constant. Thirdly, the temperature of the UCZ zone was assumed to be close to the ambient temperature. Finally, the temperature was assumed to change only in the vertical direction. It was concluded that if the NCZ is thin the heat loss will be large and that will affect the efficiency of the pond. On the other hand, if it is very thick, that will decrease the amount of insolation which reaches the LCZ significantly.

Wang and Akbarzadeh (1983) used the same steady state heat conduction equation with a slight modification. They allowed the ground temperature below the bottom of the pond at a depth of $(D_i + D_g)$ to be equal to the average ambient temperature (T_a). The heat loss to the ground was therefore taken into account in this model with two different types of soil below the pond. The value of the refraction parameter F_r was considered to be constant

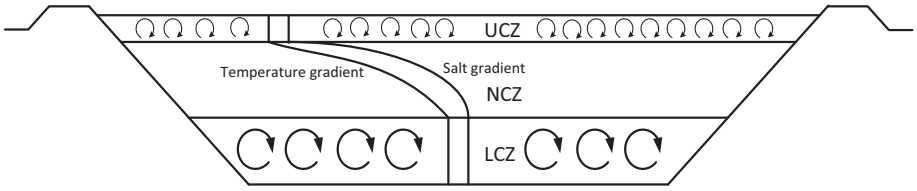

Fig. 2. The most common shape of solar pond (Leblanc et al., 2011).

(0.85) by Wang and Akbarzadeh (1983) in their model. Wang and Akbarzadeh (1983) defined the efficiency of the pond as:

$$E = \frac{q}{H} \tag{1}$$

It was observed that, if the thickness of the UCZ is decreased from 0.2 to 0.1 m, the efficiency will increase from 18.5% to 19.7%. On the other hand, if it reaches 0.5 m, the efficiency will drop to 15.5%. It was also noticed that the efficiency increases with the increase of depth of the LCZ until a maximum value is reached. Thus, a further increase will lead to the efficiency declining. Consequently, it was recommended (Wang and Akbarzadeh, 1983) that the UCZ should be kept as thin as possible and the LCZ depth should be varied depending on the desired operating temperature, to achieve the maximum efficiency. Alagao et al. (1994) discussed a closed cycle salt gradient solar pond (CCSGSP) with details. The surface water was flushed to an evaporation pond (EP), in this pond; the water solution was concentrated and re-injected at the bottom of the solar pond. It was concluded that construction a CCSGSP depends on the net of evaporation and cost of salt and land. Alagao (1996) described the transient behaviour of solar pond with complete salt recycling system. The results showed (Alagao (1996) that area of the evaporation pond in a CCSGSP operation was affected by the rate of salt transport throughout the solar pond. In recent years, other models have been developed; most of them were solved numerically. For example, Jaefarzadeh (2004) used a Crank–Nicolson scheme to solve the equations. Satisfactory results were achieved in the prediction of the temperature of the LCZ. Moreover, Andrews and Akbarzadeh (2005), investigated an alternative method of heat extraction from the SGSP; they studied heat extraction from the gradient layer (NCZ). It was concluded that heat extraction from the NCZ has the potential to increase the efficiency of the SGSP compared with the method of heat extraction from the LCZ only. Another model has been suggested by Date et al. (2013). A one-dimensional finite difference was used to solve the equations for the temperature development of the SGSP, with and without heat extraction. Safwan et al. (2014) also used the one-dimensional finite difference to solve mass and heat equations which were derived in their model.

3. Proposed model

In the present study, a model for a SGSP has been developed to solve the non-linear first order differential equations for conservation of energy. It depends on the ode45 MATLAB function which uses a modified 4th order Runge–Kutta numerical method with variable time stepping in the solution. Several assumptions have been adopted. Firstly, the pond consists of three zones; (i) the upper convective zone which contains approximately fresh water, (ii) the non-convective zone which has a gradual variation in salt concentration from top to bottom, and finally, (iii) the lower convective zone, where the concentration of salt is very high (about 0.26 kg/l). Secondly, both the UCZ and LCZ are considered well mixed. Thirdly, the solar radiation which reaches the LCZ is totally absorbed in this layer and heat accumulation in the NCZ has been neglected in the calculation of temperatures in the LCZ and UCZ. Finally, the solar insolation data from NASA has been considered and the value of refractive index $F_r = 0.85$ as was taken by Wang and Akbarzadeh (1983).

3.1. Upper convective zone (UCZ)

The upper convective zone of the pond is represented schematically in Fig. 3.

The heat conservation equation is given as:

$$\rho_u c_{pu} A_u X_u \frac{dT_u}{dt} = Q_{ru} + Q_{ub} - Q_{uc} - Q_{ur} - Q_{ue} - Q_w \tag{2}$$

The left hand side of Eq. (2) represents the useful heat accumulated in the upper convective zone. For the right hand side of the equation, Q_w is the heat loss through walls of the pond. In this work $Q_w = 0$ (i.e. it is supposed that walls are well insulated), Q_{ru} is the solar radiation that is absorbed through the upper layer. It can be calculated as:

$$Q_{ru} = Q_{r\,in} - Q_{r\,out} \tag{3}$$

where $Q_{r\,in}$ is the incident solar radiation on the pond's surface (H) and $Q_{r\,out}$ represents the solar radiation which comes out the UCZ. The value of Q_{ru} changes with time and varies with pond location. The incident radiation can be directly recorded from climatological data for any place, and it also can be calculated. In the present study data from NASA has been considered (NASA, 2014). Some of the incident sunlight reflects back to the sky and the rest of solar radiation is absorbed by the water body. Rabl and Nielsen (1975) claim that the absorption of solar radiation through a body of water cannot be described by a simple exponential. They determined the absorption coefficients and fractions of solar radiation for each of four bands. An alternative, simpler formula was suggested by Bryant and Colbeck (1977) as:

$$h_x = H(a - b \ln x) \tag{4}$$

where $a = 0.36$, $b = 0.08$, x is the thickness of water layer in meters and it is valid from 0.01 to 10 m water depth, and h_x is the solar radiation in any depth of water. That means

$$h_x = H(0.36 - 0.08 \ln x) \tag{5}$$

Eq. (5) has been used to compute the absorption solar radiation in the water body in this work, thus

$$Q_{ru} = H(1 - 0.36 + 0.08 \ln X_u) \tag{6}$$

The heat transfer to the UCZ by conduction from the LCZ is calculated by using the following equation:

$$Q_{ub} = U_t A_u [T_s - T_u] \tag{7}$$

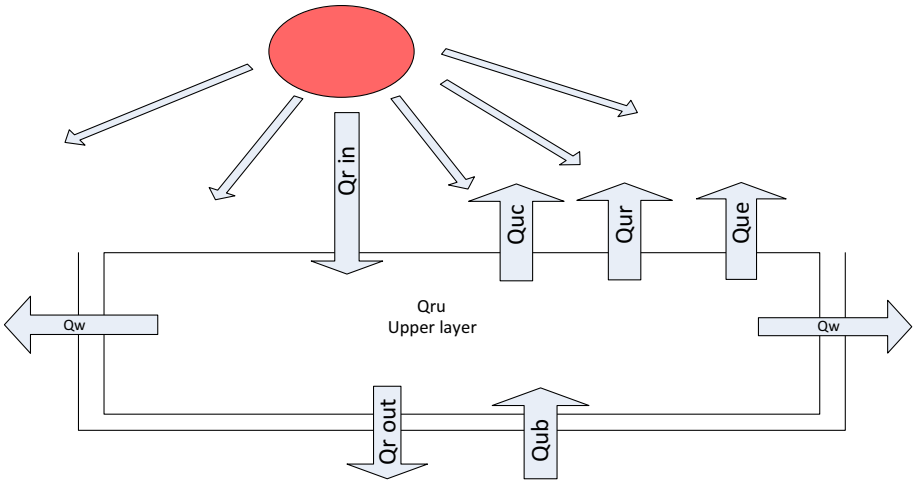

Fig. 3. Heat balance on upper layer.

Here, T_u and T_s are the temperatures of the UCZ and the LCZ respectively, and U_t is the overall heat transfer coefficient, which can be computed as:

$$U_t = \frac{1}{R_{total}} = \frac{1}{\frac{1}{h_1} + \frac{X_{NCZ}}{k_w} + \frac{1}{h_2}} \tag{8}$$

In the equation above, h_1 and h_2 are the convective heat transfer coefficient between the NCZ and the UCZ, and between the LCZ and the NCZ. Their values are 56.58 and 48.279 W/m^2 K, respectively. The thermal conductivity of water (k_w) is 0.596 W/m K (Bansal and Kaushik, 1981). The values of heat transfer coefficients were calculated theoretically by Bansal and Kaushik (1981).

Eq. (7) can therefore be written as:

$$Q_{ub} = \frac{A_u[T_s - T_u]}{\frac{1}{h_1} + \frac{X_{NCZ}}{K_w} + \frac{1}{h_2}} \tag{9}$$

The symbols Q_{uc}, Q_{ur} and Q_{ue} represent heat which is lost from the surface which can be written as:

$$Q_{loses} = Q_{uc} + Q_{ur} + Q_{ue} \tag{10}$$

Heat loss by convection Q_{uc} is given as:

$$Q_{uc} = h_c A_u[T_u - T_a] \tag{11}$$

Here h_c is the convective heat transfer coefficient from the water surface to the air in W/m^2 K and it is calculated by using a formula which was introduced by McAdams (1954) as:

$$h_c = 5.7 + 3.8v \tag{12}$$

where v is the average wind speed.

Radiation heat loss can be calculated as:

$$Q_{ur} = \sigma \in A_u(T_u^4 - T_k^4) \tag{13}$$

where σ is the Stefen–Boltzmann's constant, ϵ is the emissivity of water = 0.83 (Safwan et al., 2014), and T_k is the sky temperature. It is calculated as:

$$T_k = 0.0552T_a^{1.5} \tag{14}$$

Finally, the heat loss from the surface by evaporation (Q_{ue}) is given by Kishore and Joshi (1984) as:

$$Q_{ue} = \left\{\frac{[\lambda h_c(p_u - p_a)]}{[(1.6C_s p_{atm})]}\right\} A_u \tag{15}$$

where C_s is the humid heat capacity of air in kJ/kg. K given by:

$$C_s = 1.005 + 1.82\gamma_h \tag{16}$$

The symbol p_u is the water vapour pressure at the upper layer temperature in mmHg and it is calculated as:

$$p_u = \exp[18.403 - 3885/(T_u + 230)] \tag{17}$$

The partial pressure of water vapour in the ambient temperature in mmHg is represented by p_a and it is calculated as:

$$p_a = \gamma_h \exp[18.403 - 3885/(T_a + 230)] \tag{18}$$

Eq. (2) which represents energy conservation in the UCZ can therefore be rewritten as:

$$\rho_u c_{pu} A_u X_u \frac{dT_u}{d_t} = A_u \left[Q_{ru} + \frac{[T_s - T_u]}{\frac{1}{h_1} + \frac{X_{NCZ}}{K_w} + \frac{1}{h_2}} - \{(5.7 + 3.8v)[T_u - T_a]\} - 4.708 \times 10^{-8}\left\{T_u^4 - [0.0552(T_a)^{1.5}]^4\right\} - [\lambda h_c(p_u - p_a)]/[(1.6C_s p_{atm})] \right] \tag{19}$$

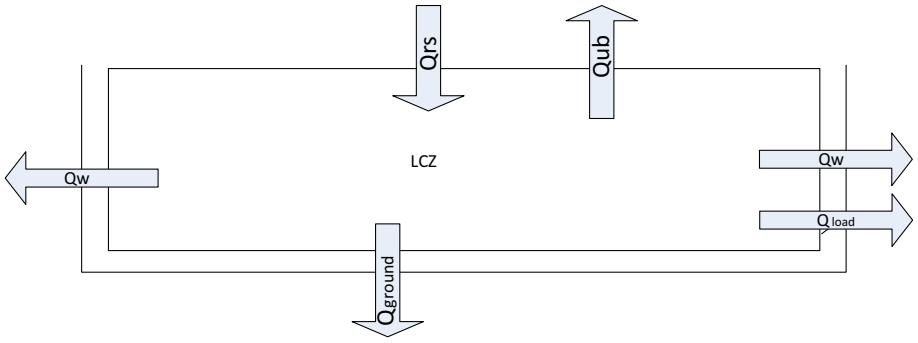

Fig. 4. Heat balance on lower convective zone (storage zone).

There are two variables in Eq. (19), i.e. T_u and T_s. Another equation with the same variables is required to find values of the unknowns. A conservation equation for energy in the storage or lower convective zone (LCZ) must also be defined.

3.2. Lower convective zone (LCZ)

The heat balance on the LCZ is illustrated in Fig. 4.
A heat balance on the LCZ is given as:

$$\rho_l c_{pl} A_l X_l \frac{dT_s}{dt} = Q_{rs} - Q_{ub} - Q_{ground} - Q_{load} - Q_w \tag{20}$$

It is assumed to begin with that there is no load i.e. $Q_{load} = 0$. This corresponds to the initial warming period of the pond. In addition, it is assumed that $Q_w = 0$ i.e. it is supposed that walls are well insulated. Eq. (20) can be rewritten as:

$$\rho_l c_{pl} A_l X_l \frac{dT_s}{dt} = Q_{rs} - Q_{ub} - Q_{ground} \tag{21}$$

The solar radiation which enters and is stored in the LCZ (Q_{rs}) can be computed by using Eq. (5), and in this case:

$$Q_{rs} = H_{LCZ} = H(0.36 - 0.08\ln(X_u + X_{NCZ}) \tag{22}$$

Heat which moves upward from the LCZ (Q_{ub}), can be calculated from Eq. (9). This is considered to be the same as the heat that moves to the UCZ.
To calculate Q_{ground}, the equation is:

$$Q_{ground} = U_{ground} A_b (T_s - T_g) \tag{23}$$

The overall heat transfer coefficient to the ground is given as:

$$U_{ground} = \frac{1}{R_3 + R_g + R_4} \tag{24}$$

The symbols R_3, R_g and R_4 represent the resistances to heat transfer to the ground.

$$R_3 = \frac{1}{h_3},\ R_g = \frac{x_g}{k_g},\ R_4 = \frac{1}{h_4}$$

Here h_3 is the convective heat transfer coefficient at the boundary between the storage zone and the surface at the bottom of the pond in $W/m^2\,K$, h_4 is the convective heat transfer coefficient at the surface of the ground water sink. Their values are 78.12 and 185.8 $W/m^2\,K$ respectively (Sodha et al., 1980). They were calculated theoretically by the researchers from the standard expressions of McAdams (1954). Eq. (23) becomes:

$$Q_{ground} = \frac{A_b(T_s - T_g)}{\frac{1}{h_3} + \frac{x_g}{k_g} + \frac{1}{h_4}} \tag{25}$$

Hull et al. (1984) claim that heat loss from any pond to the ground is a function of both perimeter and area of the pond. It also depends on the conductivity of the soil and distance to the water table beneath the pond. Their conclusion was based on many experiments and numerical simulations. Hull et al. (1988) assumed that the temperature of the water table under the pond is constant and proposed a new equation to model this transfer.

$$U_{ground} = \frac{k_g}{x_g} + m k_g \frac{p}{A_u} \tag{26}$$

The value of empirical parameter (m) varies depending on whether the walls of the pond are vertical or inclined. Eq. (23) can be re-written including this formulation as:

$$Q_{ground} = \left\{ \left(\frac{k_g}{x_g} + m k_g \frac{p}{A_u} \right) A_b (T_s - T_g) \right\} \tag{27}$$

In the present study another case for the pond has been considered. It is supposed that the pond is unburied; i.e. it is above ground with a space between it and the ground. It is suggested that bottom of the pond consists of three layers, two layers of wood and a layer of polystyrene between. In this situation U_{ground} can be given as.

$$U_{ground} = 1 \Big/ \left[\left(\frac{1}{h_3}\right) + \left(\frac{l_1}{k_1}\right) + \left(\frac{l_2}{k_2}\right) + \left(\frac{l_3}{k_3}\right) + \left(\frac{1}{h_o}\right) \right] \tag{28}$$

In Eq. (28), l_1, k_1 are the thickness and thermal conductivity of the first layer of insulation (wood). Their values are 0.01 m and 0.13 W/m K respectively. Similarly, l_2, k_2 are

the thickness and thermal conductivity for the second layer of insulation (polystyrene). Their values are 0.06 m and 0.03 W/m K respectively. Finally, l_3, k_3 are the thickness and thermal conductivity for the third layer of insulation. Their values are similar to l_1 and k_1. The heat transfer coefficient from the outside surface to the atmosphere (h_o) is taken as 5.43 W/m^2 K.

Eq. (23) will be:

$$Q_{ground} = \left[\frac{1}{\left[\left(\frac{1}{h_3}\right)+\left(\frac{l_1}{k_1}\right)+\left(\frac{l_2}{k_2}\right)+\left(\frac{l_3}{k_3}\right)+\left(\frac{1}{h_o}\right)\right]}\right] A_b(T_s - T_a) \tag{29}$$

Eq. (20) can be rewritten as:

$$\rho_l c_{pl} A_l X_l \frac{dT_s}{dt} = A_l \left[Q_{rs} - \frac{[T_s - T_u]}{\frac{1}{h_1}+\frac{X_{NCZ}}{K_w}+\frac{1}{h_2}} - Q_{load}\right] - \frac{A_b(T_s - T_g)}{\frac{1}{h_3}+\frac{x_g}{k_g}+\frac{1}{h_4}} \tag{30}$$

Hence, three different expressions have been used in Eq. (30) to represent Q_{ground}. For three or four months Q_{load} can be neglected to give the pond time to warm up.

4. Results and discussion

Eqs. (19) and (30) have been solved by using MATLAB. Three different formulae for Q_{ground} were used and different results have been observed. By this method Eqs. (19) and (30) can be solved depending on the initial values of the unknown temperatures T_u and T_s. These initial values vary with the location of the pond and the time of year when the pond starts working. The values of the constants which are used in the model are as follows $\rho_u = 1000$ kg/m^3, $\rho_l = 1200$ kg/m^3, $c_{pu} = 4180$ J/kg K, $c_{pl} = 3300$ J/kg K, $A_u = A_l = A_b = 1$ m^2, $h_1 = 56.58$, $h_2 = 48.279$, $h_3 = 78.12$, $h_4 = 185$ (all values in W/m^2 K) and $k_w = 0.596$ W/m K, $T_g = 23$ °C. The value of x_g and k_g depends on the soil properties under the pond, for example their values in El Paso pond in the USA are different from values for Ein Boqeq pond in Israel. The effect of evaporation, radiation and convection on the pond has been investigated, and values of solar radiation can be changed according to the location. The pond is first considered to be in Kuwait to compare results with available experimental data for this city. The climatic conditions for Kuwait City are listed in Table 1.

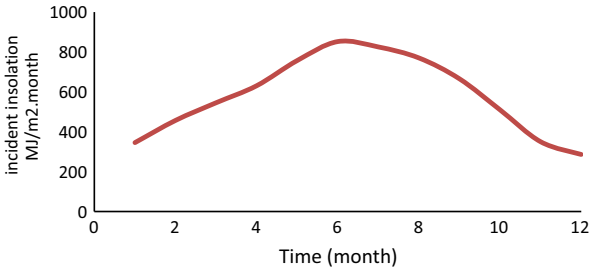

Fig. 5. Profile solar radiation of Kuwait City during one year.

It is beneficial to plot the profile of the incident solar radiation in the location of the pond to observe its behaviour during the year. The radiation profile can help to observe easily the changes in the radiation throughout the year and to identify when it is high or low. The profile appears in Fig. 5 for Kuwait City.

It is clear from Fig. 5 that the incident solar radiation on this city increases gradually from the winter to the summer season and it reaches the maximum value in June. There is clearly a very large seasonal range in the insolation, which will significantly affect the behaviour of the pond.

4.1. Validation of the model

4.1.1. Kuwait city

To examine the validity of the model, the computed temperature of the LCZ is compared with the experimental data of Ali (1986) for a pond in Kuwait city (there was no heat extraction from the pond). The dimensions of the Kuwait pond were 4 × 2 × 0.9 m and the depth of layers

Table 1
Climatic conditions of Kuwait city (NASA, 2014).

Month	Solar radiation (MJ/m^2 month)	Ambient temperature (°C)	Relative humidity (%)	Wind speed (m/s)
January	345.6	12.6	53.6	3.3
February	456.84	14.6	43.7	3.5
March	545.4	19.1	37.9	3.7
April	630.72	25.9	29	3.4
May	757.08	32	20.4	4.1
June	852.12	35.7	15.3	4.5
July	825.12	37.6	15.2	4.2
August	770.04	37.2	17.4	4.1
September	665.28	33.6	20.6	3.7
October	509.76	28.1	30.1	3.3
November	349.92	20.5	43.2	3.4
December	286.2	14.7	51.5	3.4
Average	514.08	25.96	31.49	3.7

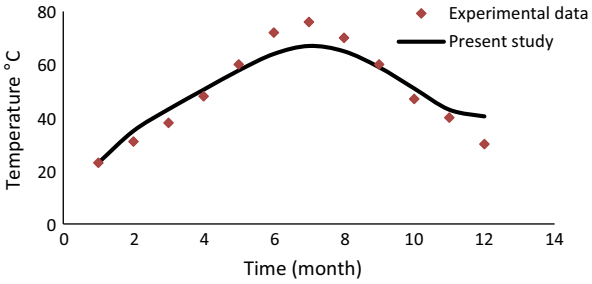

Fig. 6. Validation of temperature distribution of the LCZ of the present model with experimental data for Kuwait City (initial temperatures are 14 and 23 °C for the UCZ and LCZ respectively).

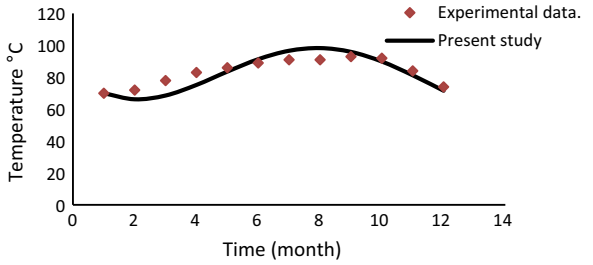

Fig. 7. Comparison profiles of the LCZ temperature of the present model with El-Paso pond experimental data (1999) (initial temperatures are 6 and 70 °C for UCZ and LCZ respectively).

was 0.2, 0.4 and 0.3 m for UCZ, NCZ and LCZ respectively. This comparison is shown in Fig. 6.

There is a good agreement between the model and experimental data for the temperature in the storage zone. A slight variation in temperatures of the LCZ is apparent. This variation might be due to the difference between real and assumed values of the heat transfer coefficients.

4.1.2. El Paso

The present model is also compared with experimental data from the El-Paso solar pond (1999), (with these experimental results there was also no load). The surface area of this pond is 3000 m^2 and the depths of layers are 0.7, 1.2 and 1.35 m for UCZ, NCZ and LCZ respectively (Huanmin et al., 2001). The depth is large compared with the Kuwait solar pond. The climatic conditions of El Paso are shown in Table 2 and the comparison is demonstrated in Fig. 7.

The profile of the experimental measurement in the LCZ tends to show little variation in the temperature. This slight variation might be due to the high initial temperature because it has an effect on the behaviour of temperature in the LCZ. This effect has been discussed by many researchers e.g. Jaefarzadeh (2004, 2005) and Madani (2014). It was concluded that the initial temperature has a slight effect on the LCZ temperature and after few months the difference in maximum temperature among cases with different initial temperatures becomes low. In other words, if two ponds start with two different temperatures for the LCZ with one of them being low and the other one high, then the temperature in the LCZ in the first one will increase while in the second one temperature will decrease slightly. Subsequently it will increase slowly as the radiation intensity increases. However, after few months the gap between the two temperatures will be small. As demonstrated in Fig. 7, for the model, the behaviour is approximately similar to the described behaviour because before May, the temperature decreases, after that it increases gradually. It reaches maximum value in August. A gradual decrease in temperature is seen after August to be close to the experimental results. The difference between the two values of temperatures becomes very small from September. The difference between the experimental data of the El Paso pond and theoretical values according to the present study may be because of the difference between theoretical and experimental heat transfer coefficient, but also the clarity of the pond because it was working for a long time prior to the measurements in 1999.

4.2. Effect of ground heat loss

The experimental data for the LCZ of Ali's (1986) pond in Kuwait is also compared with the present model, but by using Eqs. (27) and (29) to represent heat loss to the ground, comparison is illustrated in Fig. 8.

It is apparent from Fig. 8 that in the case of an unburied pond (Eq. (29) has been used for Q_{ground}). The temperatures

Table 2
Climatic conditions of El Paso, Texas (1999), (Huanmin et al., 2001).

Month	Solar radiation (MJ/m^2 month)	Ambient temperature (°C)	Relative humidity (%)	Wind speed (m/s)
January	378	6	51	3.2
February	486	8.9	42	3.5
March	637	12.8	32	4.4
April	766	17.4	27	4.4
May	842.4	22.1	27	4.1
June	864	26.9	30	3.5
July	799	27.9	44	3.2
August	734	26.7	48	3
September	637	23.6	51	2.9
October	529	17.8	47	2.8
November	410	11.3	47	3.1
December	345	6.7	52	3
Average	618	17.3	41.5	3.4

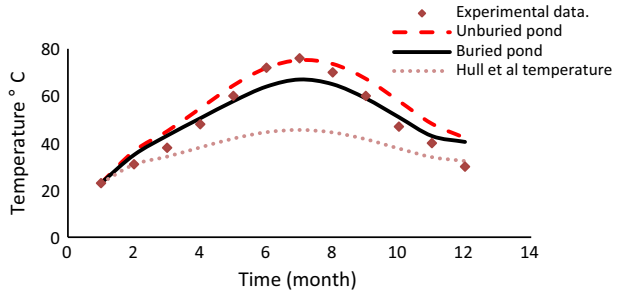

Fig. 8. Comparison of experimental temperature distribution of the lower layer LCZ of the Kuwait pond with unburied and Hull et al. (1988) formulae for heat loss to the ground.

are higher than the experimental values for most of the year. This difference can be explained by two facts. Firstly, the buried pond in the present model loses heat to the ground because the shallow layers of soil have high thermal conductivity. Consequently, heat loss to the soil from the bottom of the pond (no heat loss from walls, as they are considered well insulated) is higher than in the unburied case and has an impact on the pond, causing a decrease in temperature. Secondly, the temperature of the air reaches more than 37 °C in some areas, particularly in arid and desert places including Kuwait (Table 2). In this situation heat loss to the atmosphere in the proposed unburied pond will be small as compared with the buried pond with continuous heat loss to the soil. The profile of the LCZ in the case of unburied pond gives an indication that this pond can reach a temperature higher than a buried pond during the year, particularly, in hot areas. However, new parameters will appear in this case and need to be tackled. An economic balance will be very helpful to evaluate the positive and negative factors. These factors can be discussed economically and experimental data can provide guide for this type of pond.

When heat loss to the ground is computed by applying the formula which is proposed by Hull et al. (1988), it is obvious from Fig. 8 that the increases in temperature are slower than the experimental changes. The reason for this behaviour is probably the effect of perimeter because Hull et al. consider it has high impact on the temperature of the pond. That effect can be observed from the formula of Hull et al. (1988) in Eq. (26) for U_{ground}.

$$U_{ground} = \frac{k_g}{x_g} + mk_g \frac{p}{A_u} \tag{31}$$

The suggested formula illustrates mathematically that the second term has significant influence on the value of U_{ground} for small ponds because the contribution of $\frac{p}{A_u}$ is important. In large ponds the influence of $\frac{p}{A_u}$ will decrease substantially. To investigate this situation, a pond of the same depth as the Kuwait pond $2 \times 4 \times 0.9$ m, but with different dimensions $30 \times 100 \times 0.9$ m has modelled and compared with the small pond. The specifications of the two ponds are shown in Table 3.

It is clear from Table 3 that the difference between ponds is only in surface area and perimeter. The profiles of temperature for both ponds are demonstrated in Fig. 9.

Fig. 9 demonstrates that temperature of the suggested large pond with 3000 m^2 of surface area and 260 m perimeter is much higher than the temperature of the small pond 8 m^2 and 12 m perimeter throughout the year. The shape of the pond can be significant because perimeter changes with geometrical shape. The temperature can also increase by increasing the depth of the pond because the selected layer's depth is small (0.2, 0.4, 0.3) m for UCZ, NCZ and LCZ respectively.

4.3. Temperature distributions in suggested model pond

4.3.1. Temperature profiles in the UCZ and LCZ

The profiles of temperature for both upper and lower layers have been plotted for a pond with dimensions of $1 \times 1 \times 1.5$ m and thicknesses of 0.2, 0.8 and 0.5 m for the UCZ, NCZ and LCZ respectively. Once again the pond is assumed to be in Kuwait City. The profiles are shown in Fig. 10.

It is obvious from Fig. 10 that the temperature of the lower layer increases substantially with time to reach maximum values around 90 °C during July. After that the temperature decreases slightly with time to remain between 50 and 60 °C in December. The reason for this behaviour is that solar radiation incident on the pond also increases steadily in the first part of the year and it reaches the highest value in June. In the latter half of the year the radiation decreases. This behaviour can be seen apparently in Fig. 5. It is approximately clear from Fig. 10 that the temperature of the LCZ is around 50–60 °C in the end of the year even with cold weather in winter. This is due to the accumulation of heat. Moreover, heat loss from the walls is neglected and that means the pond might remain warm for a long

Table 3
Small and large suggested pond specifications.

	Location	Dimensions (m)	Layer depth (m) UCZ, NCZ, LCZ
Small pond	Kuwait	$4 \times 2 \times 0.9$	0.2, 0.4, 0.3
Large pond	Kuwait	$30 \times 100 \times 0.9$	0.2, 0.4, 0.3

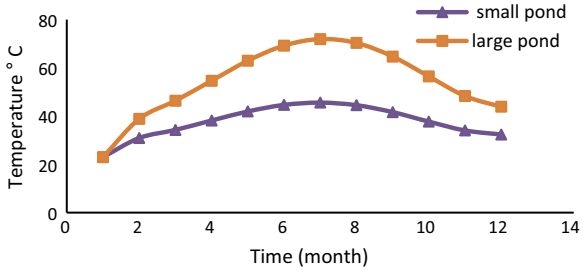

Fig. 9. Comparison of temperature distribution of lower layer (LCZ) between small and large pond when formula of Hull et al. (1988) is used.

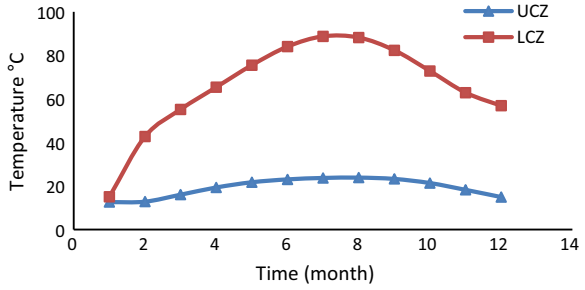

Fig. 10. Profile of temperature in LCZ and UCZ during one year (initial temperatures are 12.6 °C for both layers and month 1 is January).

time. The variation of upper layer temperature is small. This is as a consequence of heat exchange between water surface and the surrounding air and that leads to the temperature of UCZ tending to the air temperature. Similar behaviour has been observed by many researchers, e.g. Safwan et al. (2014), Alenezi (2012), Srinivasan (1993), Al-Jamal and Khashan (1998), Date et al. (2013), Karakilcik et al. (2006), Garman and Muntasser (2008) and Jaefarzadeh (2005).

4.3.2. Non-convective zone

The temperatures of NCZ have also been calculated for every month by dividing the layer into many layers. The thickness of every layer is chosen as 0.1 m. Fig. 11 shows the NCZ layer.

An energy balance on every layer in the NCZ layer can be written as:

$$Q = K_w \frac{\partial T}{\partial x} + Q_R \tag{31}$$

The energy transferred through the NCZ by conduction is computed by;

$$Q = U_t \Delta T \tag{32}$$

The overall heat transfer coefficient U_t is calculated by applying Eq. (8). The distribution of temperature through the NCZ can be calculated for any month during the year

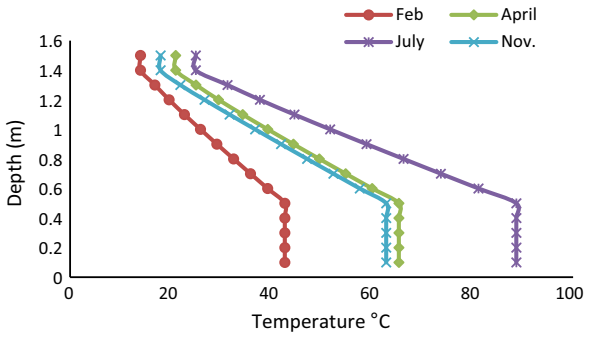

Fig. 12. The distribution of temperature in the pond for four selected month, February, April, July and November.

and it can be started form the upper or lower layer. The profile of temperature for the whole pond can be drawn through any month of the year. It is illustrated in Fig. 12 for four months.

As shown from Fig. 12, temperature is constant in both upper and lower layer because the two layers are considered well mixed in the model. The temperature of the middle layer (NCZ) decreases gradually from the bottom to the top of the pond. The same behaviour is observed in both experimental and theoretical studies on the salt gradient solar pond. The highest difference between temperature in the LCZ and UCZ is in July (more than 60 °C) whereas the lowest is in February (less than 30 °C).

4.4. Surface heat loss

The rate at which heat is lost from the surface of the pond obviously plays a significant role in determining its performance. Three heat loss mechanisms operate in parallel, namely radiation, convection and evaporation. To assess the importance of each of these mechanisms, each was considered to occur in isolation. The effect of this mechanism for heat loss on the performance of the pond could then be ascertained by inspection of the temperatures

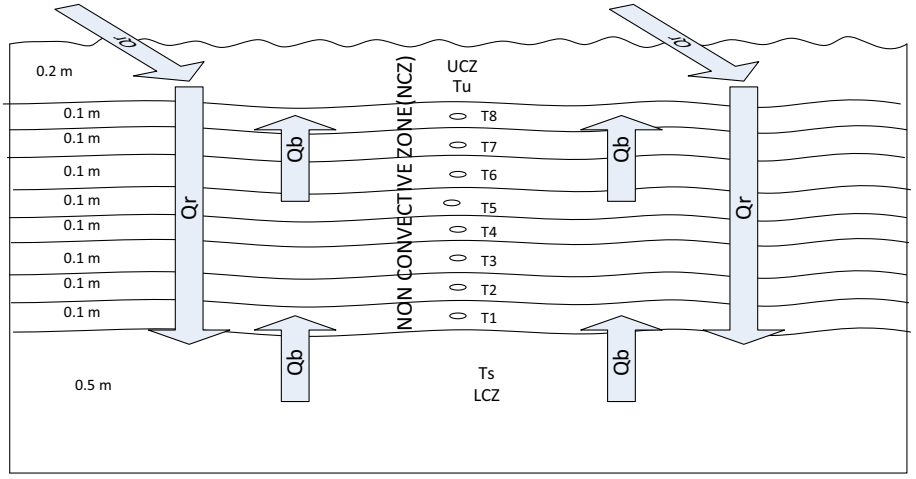

Fig. 11. NCZ section of the pond which shows the suggested partitions.

reached in the pond. Firstly, evaporation and convection have been neglected to observe the effect of radiation only. The same process is repeated for evaporation and convection. It is appear that evaporation has the highest influence on both LCZ and UCZ temperatures. In contrast radiation has the lowest effect on both temperatures. Convection has also a substantial effect on both temperatures. Data is plotted and shown in Figs. 13 and 14 for the LCZ and UCZ respectively.

It is apparent from the two figures that when only radiation is considered, the temperatures of both the storage layer and upper layer reach high (and obviously unphysical) values and that means it has a small effect on the temperature of the UCZ and the LCZ. With evaporation temperatures in the UCZ and LCZ become low; the lowest values for the temperature in both layers (UCZ and LCZ) are observed with only evaporation case. For the UCZ, the temperature in case of evaporation only is lower than temperature when three types of heat loss are considered. To explain this behaviour it is helpful to plot the ambient temperature in area of the pond (Kuwait) with the temperature of the UCZ. The profiles of both temperatures are illustrated in Fig. 15.

It can be seen that the ambient temperature is higher than the temperature of the UCZ for most months during the year. That means heat could be transferred from the atmosphere to the pond according to Eq. (11). In the El-Paso pond it is observed that ambient temperature is higher than upper layer temperature of the pond for most months through one year (Huanmin et al., 2001). The data which published by the researchers is plotted and demonstrated in Fig. 16.

It is clear from Fig. 16 that ambient temperature is higher than temperature of the upper layer. The difference continues from the first month to October when it becomes very small. Evaporation even occurs at temperatures lower than ambient temperature. With all cases there is an energy which is added from the surrounded air, but with evaporation only, there is no heat addition.

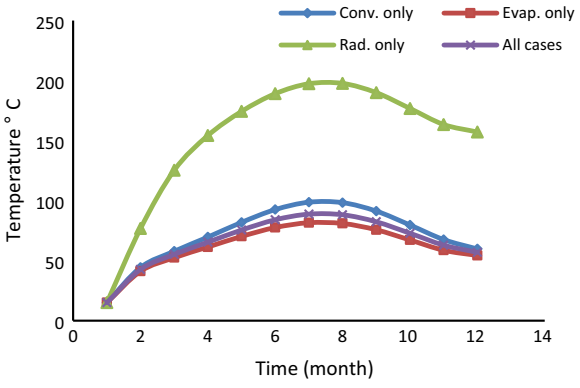

Fig. 13. Temperature of the LCZ with different cases of heat loss from the surface.

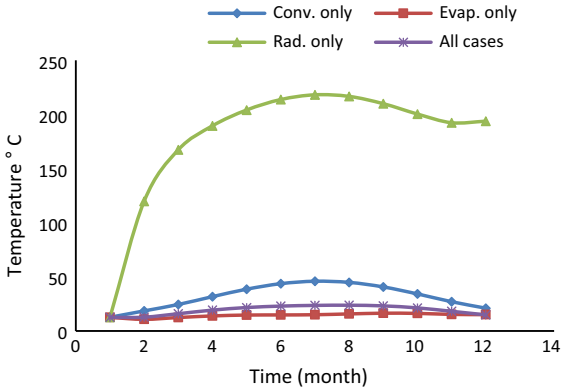

Fig. 14. Temperature of the UCZ with different cases of heat loss from the surface.

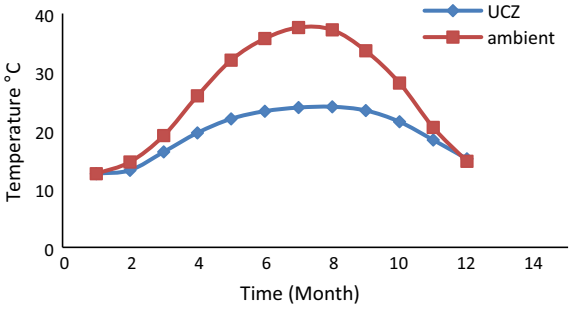

Fig. 15. Profiles of both the ambient and the calculated temperatures of UCZ.

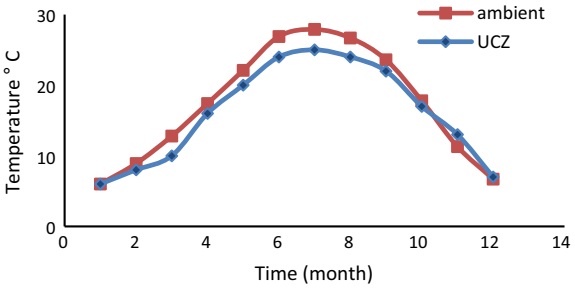

Fig. 16. Profiles of both measured ambient and UCZ temperatures for El-Paso pond (1999), extracted from Huanmin et al. (2001).

5. Conclusion

This paper has presented a model to calculate temperature in the three zones of a SGSP. The results are validated by comparison with experimental data and a good agreement has been obtained. It is noticed that temperature of a model pond in Kuwait reaches around 90 °C in July and decreases to around 50 °C at the end of the year. Obviously, a solar pond can supply heat temporarily during the year, even in winter with cloudy and cold weather, but it needs time to warm up. In the unburied ponds, temperature in the LCZ is higher than normal buried pond. It is concluded that perimeter has a significant effect on the LCZ tempera-

ture in the case of the small ponds, whereas the effect is unsubstantial in the case of the large ponds. Consequently, the shape of the small pond is important because perimeter changes with shape. The relative importance of evaporation, convection and radiation heat loss from the surface has been investigated. It is found that heat loss from surface by evaporation has the largest effect on the temperature of the LCZ whereas radiation has the smallest impact. Studies on evaporation and trying to decrease its impact will be useful and they might significantly increase efficiency of the salt gradient solar pond.

References

AbdelSalam, M., 1985. A multipurpose shallow solar pond (MSSP). Sol. Wind Technol. 1 (3), 167–174.

Alagao, F.B., 1996. Simulation of the transient behaviour of a closed-cycle salt-gradient solar pond. Sol. Energy 56 (3), 245–260.

Alagao, F.B., Akbarzadeh, A., Johnson, P., 1994. The design, construction, and initial operation of closed-cycle salt gradient solar pond. Sol. Energy 53, 343–351.

Alenezi, I., 2012. Salinity Gradient Solar Ponds: Theoretical Modelling and Integration with Desalination. PhD's Thesis, University of Surrey. <http://epubs.surrey.ac.uk/745998/1> (accessed 15 February 2014).

Ali, H.M., 1986. Mathematical modelling of salt gradient solar pond performance. Energy Res. 10, 377–384.

AL-Jamal, K., Khashan, S., 1998. Effect of energy extraction on solar pond performance. Energy Convers. Manage. 39 (7), 559–566.

Alrowaished, A., Azni, I., Mohamed, Thamer A., Amimul, A., 2013. The development and applications of solar pond: a review. Desalination Water Treat. 10, 1–13.

Anderson, A.L., 1980. Solar pond what are they? Second Industrial Energy Technology Conference. Houston, TX, 13–16 April.

Andrews, J., Akbarzadeh, A., 2005. Enhancing the thermal efficiency of solar ponds by extracting heat from the gradient layer. Sol. Energy 78 (6), 704–716.

Bansal, P.K., Kaushik, N.D., 1981. Salt gradient stabilized solar pond collector. Energy Convers. Manage. 21, 81–95.

Benjamin Schober, 2010. Membrane Stratified Solar Ponds. Master's Thesis, University of Gavle. <http://www.diva-portal.org/smash/get/diva2:326646/FULLTEXT01> (accessed 20 February 2014).

Bryant, H.C., Colbeck, I., 1977. A solar pond for London?. Sol. Energy 19 (3) 321–322.

Date, A., Akbarzadeh, A., 2013. Salinity gradient solar ponds. In: Napoleon, E., Akbarzadeh, A. (Eds.), Energy Sciences and Engineering Applications. CRC press. E. Book.

Date, A., Yusli, Y., Ashwin, D., Shankar, K., Akbarzadeh, A., 2013. Heat extraction from non-convective and lower convective zones of the solar pond: a transient study. Sol. Energy 97, 517–528.

Garg, H.P., 1987. Advance in Solar Energy Technology, Collection and Storage Systems. Springer, Holland.

Garman, M.A., Muntasser, M.A., 2008. Sizing and thermal study of salinity gradient solar ponds connecting with MED desalination unit. Desalination 222, 689–695.

Huanmin, Lu., John, C.W., Andrew, H.P., 2001. Desalination coupled with salinity gradient solar ponds. Desalination 136, 13–23.

Huanmin, Lu., John, C.W., Andrew, H.P., Herbert, D.H., 2004. Advancements in salinity gradient solar pond technology based on sixteen years of operational experience. J. Sol. Energy Eng. 126, 759–767.

Hull, J.R., 1980. Method and Means of Preventing Heat Convection in a Solar Pond. United States Patent, No. 4, 241, 724. <http://www.google.com/patents/US4241724> (accessed 20 April 2014).

Hull, J.R., Liu, K.V., Sha, W.T., Jyoti, K., Nielsen, C.E., 1984. Dependence of ground heat loss upon solar pond size and perimeter insulation, calculated and experimental results. Sol. Energy 33 (1), 25–33.

Hull, J.R., Nielsen, C.E., Golding, P., 1988. Salinity Gradient Solar Ponds. CRC Press, Florida.

Jaefarzadeh, M.R., 2004. Thermal behaviour of a small salinity-gradient solar pond with wall shading effect. Sol. Energy 77, 281–290.

Jaferzadeh, M.R., 2005. Thermal behaviour of a large salinity-gradient solar pond in the city of Mashhad. Iran. J. Sci. Technol., Trans. Eng. 29 (B2).

Karakilcik, M., Dincer, I., Marc, A.R., 2006. Performance investigation of a solar pond. Appl. Therm. Eng. 26, 727–735.

Kishore, V.V.N., Joshi, V., 1984. A practical collector efficiency equation for non-convecting solar ponds. Sol. Energy 33 (5), 391–395.

Kooi, C.F., 1979. The steady state salt gradient solar pond. Sol. Energy 23, 37–45.

Leblanc, J., Akbarzadeh, A., Andrews, J., Huanmin, Lu., Golding, P., 2011. Heat extraction methods from salinity–gradient solar ponds and introduction of a novel system of heat extraction for improved efficiency. Sol. Energy 85, 3103–3142.

Madani, S.S., 2014. Effect of different parameters on solar pond performance. Asia Pacific J. Energy Environ. 1 (1).

McAdams, W.H., 1954. Heat Transmission, third ed. McGraw-Hill Kogakusha, Tokyo, Japan.

Surface Meteorology and Solar Energy, a Renewable Energy Resource. <https://eosweb.larc.nasa.gov (NASA)> (accessed 25 March 2014).

Nielsen, E.C., 1975. Salt-Gradient Solar Ponds for Solar Energy Utilization, Environmental Conservation. The Foundation of Environmental Conservation, vol. 2, no. 4, printed in Switzerland.

Rabl, A., Nielsen, C.E., 1975. Solar ponds for space heating. Sol. Energy 17, 1–12.

Safwan, K., Jonathan, D., Gregory, L., 2014. A simple heat and mass transfer model for salt gradient solar ponds. Int. J. Mech., Indust. Sci. Eng. 8 (1), 27–33.

Sodha, M.S., Nayak, J.K., Kaushik, S.C., 1980. Physics of shallow solar pond water heater. Energy Res. 4, 323–337.

Srinivasan, J., 1993. Solar Pond Technology. Sadhana, vol. 18, (1) (March), pp. 39–55. Printed in India.

Velmurugan, V., Srithar, K., 2008. Prospects and scopes of solar pond: a detailed review. Renew. Sustain. Energy Rev. 12, 2253–2263.

Wang, Y.F., Akbarzadeh, A., 1983. A parametric study on solar ponds. Sol. Energy 30 (6), 555–562.

Weinberg, J., Doron, B., 2010. Desalination and Water Resources, Renewable Energy System and Desalination. ISBN: 978-1-84826-430-4.

Wilkins, E., Lee, T.K., 1987. Design and optimization of the gel solar pond. Can. J. Chem. Eng., 65

Wilkins, E., El-Genk, M., El-Husseini, K., Thakur, D., 1982. An Evaluation of the Gel Pond Performance. The American Society of Mechanical Engineers, 345E. 47 St., New York, N.Y. 10017.